Reaction of Butyltin Hydroxide Oxide with *p*-Toluenesulfonic Acid: Synthesis, X-ray Crystal Analysis, and Multinuclear NMR Characterization of $\{(BuSn)_{12}O_{14}(OH)_6\}(4\text{-}CH_3C_6H_4SO_3)_2$

Christophe Eychenne-Baron, François Ribot,* Nathalie Steunou, and Clément Sanchez

Laboratoire de Chimie de la Matière Condensée, UMR CNRS 7574, Tour 54, 5e étage, Université Pierre et Marie Curie, 4 Place Jussieu, F-75252 Paris Cedex 05, France

Franck Fayon

Centre de Recherche sur les Matériaux à Haute Température, UPR CNRS 4212, 1D avenue de la Recherche Scientifique, F-45071 Orléans Cedex 2, France

Monique Biesemans, José C. Martins, and Rudolph Willem

High-Resolution NMR Center (HNMR), Free University of Brussels (VUB), Pleinlaan 2, B-1050 Brussels, Belgium

Received November 2, 1999

The reaction of butyltin hydroxide oxide, BuSnO(OH), with *p*-toluenesulfonic acid, $4\text{-}CH_3C_6H_4SO_3H$, yields the butyltin oxo cluster $\{(BuSn)_{12}(\mu_3\text{-}O)_{14}(\mu_2\text{-}OH)_6\}^{2+}$ mixed with a soluble ill-defined butyltin oxo polymer, the presence of which was established by solid-state and quantitative solution ^{119}Sn NMR. The reaction conditions were varied in order to optimize the yield of oxo cluster, which can be quantitatively isolated by crystallization as $\{(BuSn)_{12}O_{14}(OH)_6\}(4\text{-}CH_3C_6H_4SO_3)_2 \cdot C_4H_8O_2$ (**1**·diox). The structure of the latter compound was determined by X-ray diffraction. **1**·diox and $\{(BuSn)_{12}O_{14}(OH)_6\}(4\text{-}CH_3C_6H_4SO_3)_2$ (**1**) were also characterized by solid-state ^{119}Sn MAS NMR and solution ^{119}Sn, ^1H, and ^{13}C NMR. In **1**·diox, the existence of weak Lewis interactions, taking place in the crystal between five-coordinate tin atoms and dioxane molecules, was evidenced by solid-state ^{119}Sn NMR. 2D $^1H-^1H$ NOESY and ROESY experiments, along with ionic conductivity measurements, have proved that the ionic dissociation between $\{(BuSn)_{12}O_{14}(OH)_6\}^{2+}$ and $4\text{-}CH_3C_6H_4SO_3^-$ (PTS^-) does not take place in dichloromethane, while it does in the more polar and dissociating dimethyl sulfoxide. Using the $^1H-^{119}Sn$ *J*-HMQC NMR technique, the weak $^2J(^1H-O-^{119}Sn)$ coupling constant between the μ_2-OH and the six-coordinate tin nuclei was determined and shown to depend on the solvent.

Introduction

Several structures of monoorganotin oxo clusters have been shown to be versatile nanobuilding blocks for the design of tin-based hybrid organic−inorganic materials.[1] Many of these oxo clusters contain strongly complexing ligands such as carboxylates (i.e., $[PhSnO(O_2CC_6H_{11})]_6$),[2] phosphinates (i.e., $\{[BuSn(OH)(O_2PPh_2)]_3O\}(O_2PPh_2)$),[3] and phosphates (i.e., $[BuSnO(O_2P(OPh)_2)]_6$),[4] which cover the oxo cores and generally allow hexacoordination for tin. They are usually synthesized from organostannonic acids and the corresponding carboxylic- or phosphorus-based acids in a nonpolar solvent.[5] The starting Sn/acid ratio and the nature of the acid control the outcome of these syntheses. Other monorganotin oxo clusters, without complexing ligands bound to tin (i.e., $(Pr^iSn)_9O_8(OH)_6Cl_5$[6] or $\{(Pr^iSn)_{12}O_{14}(OH)_6\}Cl_2$),[7] are also known. All of these have been prepared, sometimes with very low yields, by hydrolysis−condensation of molecular monoorganotin compounds ($RSnCl_3$,[6−8] $RSn(OR')_3$,[9] or $RSn(C{\equiv}CR')_3$[10]). However, we have recently shown that the reaction of sulfonic acid with butylstannonic acid, BuSnO(OH), is a cheap and easy alternative to prepare the macrocation $\{(BuSn)_{12}O_{14}(OH)_6\}^{2+}$.[11]

* To whom correspondence should be addressed. E-mail: fri@ccr.jussieu.fr.

(1) Ribot, F.; Eychenne-Baron, C.; Sanchez, C. *Phosphorus, Sulfur Silicon Relat. Elem.* **1999**, *150−151*, 41.
(2) Chandrasekhar, V.; Day, R. O.; Holmes, R. R. *Inorg. Chem.* **1985**, *24*, 1970.
(3) Day, R. O.; Holmes, J. M.; Chandrasekhar, V.; Holmes, R. R. *J. Am. Chem. Soc.* **1987**, *109*, 940.
(4) Day, R. O.; Chandrasekhar, V.; Kumara Swamy, K. C.; Holmes, J. M.; Burton, S. D.; Holmes, R. R. *Inorg. Chem.* **1988**, *27*, 2887.
(5) Holmes, R. R. *Acc. Chem. Res.* **1989**, *22*, 190.
(6) Puff, H.; Reuter, H. *J. Organomet. Chem.* **1989**, *368*, 173.
(7) Puff, H.; Reuter, H. *J. Organomet. Chem.* **1989**, *373*, 173.
(8) Dakternieks, D.; Zhu, H.; Tiekink, E. R. T.; Colton, R. J. *J. Organomet. Chem.* **1994**, *476*, 33.
(9) Banse, F.; Ribot, F.; Tolédano, P.; Maquet, J.; Sanchez, C. *Inorg. Chem.* **1995**, *34*, 6371.
(10) Jaumier, P.; Jousseaume, B.; Lahcini, M.; Ribot, F.; Sanchez, C. *J. Chem. Soc., Chem. Commun.* **1998**, 369.
(11) Eychenne-Baron, C.; Ribot, F.; Sanchez, C. *J. Organomet. Chem.* **1998**, *567*, 137.

10.1021/om990877a CCC: $19.00
Publication on Web 04/14/2000

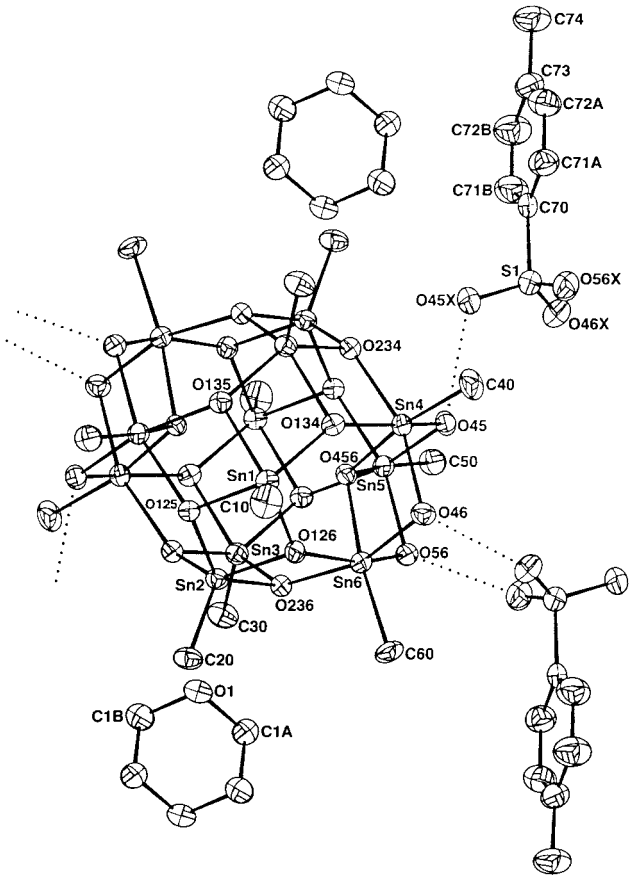

Figure 1. CAMERON[31] drawing of $\{(BuSn)_{12}O_{14}(OH)_6\}(4\text{-}CH_3C_6H_4SO_3)_2\cdot C_4H_8O_2$ (**1**·diox), showing 20% displacement ellipsoids (two dioxane molecules have been represented, but only the α-carbon of the butyl chains has been drawn for clarity).

This paper reports on the reaction between BuSnO(OH) and $4\text{-}CH_3C_6H_4SO_3H$ (HPTS), with different nominal tin-to-sulfur ratios (Sn/S varying from 12/2 to 12/8). The crystallographic structure of $\{(BuSn)_{12}O_{14}(OH)_6\}(4\text{-}CH_3C_6H_4SO_3)_2\cdot C_4H_8O_2$ (**1**·diox; diox = dioxane), as determined from single-crystal X-ray diffraction, as well as solid- and solution-state multinuclear NMR charaterizations of **1** and **1**·diox, are presented. The interactions between $\{(BuSn)_{12}O_{14}(OH)_6\}^{2+}$ and $4\text{-}CH_3C_6H_4SO_3^-$ (PTS^-) in solution were investigated.

Results and Discussion

X-ray Diffraction Structure of 1·diox. The molecular structure and a packing diagram of **1**·diox are presented in Figures 1 and 2, respectively. Selected interatomic distances and bond angles are given in Table 1. The main component of this centrosymmetric compound is the $\{(RSn)_{12}(\mu_3\text{-}O)_{14}(\mu_2\text{-}OH)_6\}^{2+}$ macrocation.[7−9]

As previously reported,[7−9] it is composed of twelve tin atoms bound to one butyl group and linked by μ_3-O (O125, O126, O134, O135, O234, O236, O456, and their symmetric counterparts) and μ_2-OH bridges (O45, O46, O56, and their symmetric counterparts). The six five-coordinate tin atoms exhibit a square-pyramidal environment (Sn1, Sn2, Sn3 and their symmetric), while the other six tin atoms exhibit a six-coordinate distorted-octahedral geometry (Sn4, Sn5, Sn6, and their symmetric counterparts). Six hydroxy groups bridge the six-coordinate tin atoms pairwise and define the cage poles.

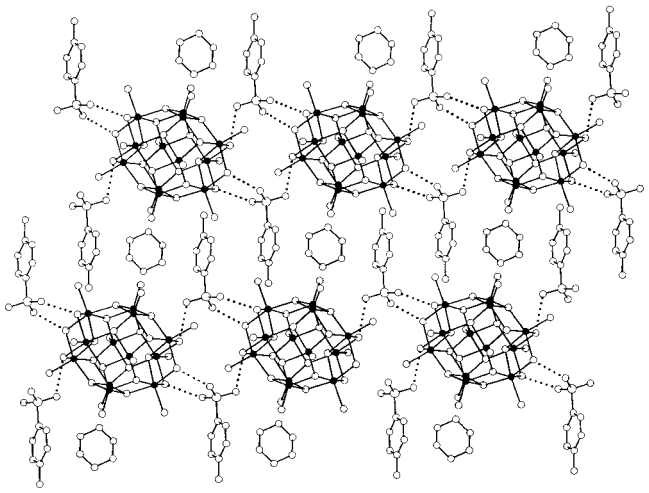

Figure 2. Packing diagram for $\{(BuSn)_{12}O_{14}(OH)_6\}(4\text{-}CH_3C_6H_4SO_3)_2\cdot C_4H_8O_2$ (**1**·diox), showing the "cation−anion" chains (parallel to [100]) and their arrangement into planes (parallel to [110]).

Two *p*-toluenesulfonate counteranions interact with the cage poles. A framework of hydrogen bonds, characterized by an average O−O distance of 2.74 Å, links the oxo clusters into chains parallel to the *a* axis of the structure (Figure 2). This framework involves one-to-one contacts between the three oxygen atoms of both sulfonate anions (O45X, O46X, O56X, and their symmetric counterparts) and all six μ_2-OH bridges. The formation of chains due to counteranions bridging two macrocations is common for the $\{(BuSn)_{12}O_{14}(OH)_6\}^{2+}$ cluster, yet **1**·diox is the first where all the bridging hydroxy groups are in contact with the anions.[8,9] This feature is in line with the almost identical environments of the six-coordinate tin atoms (Table 1), in contrast with the other structures, where two main six-coordinate environments are identified.[8,9]

The oxygen atoms of a 1,4-dioxane molecule (O1, C1A, C1B, and their symmetric counterparts) form weak donor−acceptor interactions (d(Sn−O) ≈ 3.3 Å) with four five-coordinate tin atoms (Sn2, Sn3, and their symmetric counterparts). These contacts cause a small displacement of the α-carbons (C20, C30, and their symmetric counterparts), as evidenced by the O−Sn−C angles (Table 1), and connect "cation−anion" chains into planes parallel to the *a* and *b* axes (Figure 2). This type of interaction is unreported, since in all structures described so far, the solvating molecules (DMF,[7] H_2O,[8] $HOPr^i$[9]) were always hydrogen-bound to bridging hydroxy groups not interacting with the anions.

Thermal Behavior of 1·diox. The thermogravimetric and differential thermal analyses of **1**·diox (Figure 3) reveal four weight losses between 20 and 1000 °C. The final product corresponds to SnO_2 (cassiterite),[12] as revealed by X-ray powder diffraction, and the total weight loss indicates a dioxane-deficient composition close to $\{(BuSn)_{12}O_{14}(OH)_6\}(PTS)_2(C_4H_8O_2)_{0.4}$ (exptl, 35.7%; calcd, 35.7%). The first weight loss (85 °C; weakly endothermic) corresponds to leaving dioxane and agrees well with the lack of dioxane (exptl, 1.2%; calcd, 1.2%).

(12) McCarthy, G.; Welton, J. *Powder Diffr.* **1989**, *4*, 156.

Table 1. Selected Interatomic Distances (Å) and Bond Angles (deg) for $\{(BuSn)_{12}O_{14}(OH)_6\}(4\text{-}CH_3C_6H_4SO_3)_2\cdot C_4H_8O_2$ (1·diox) with Esd's in Parentheses[a]

⟨**Sn$_p$**−**O**⟩[b]	2.087	⟨**Sn$_p$**−**O**⟩	2.027	⟨**Sn$_h$**−**O**⟩	2.115
Sn1−O125	2.071(5)	Sn1−O134	2.020(5)	Sn4−O134	2.115(5)
Sn1−O135	2.094(5)	Sn1−O126	2.026(5)	Sn4−O234	2.126(5)
Sn2−O126	2.100(5)	Sn2−O125	2.043(5)	Sn5−O125′	2.097(5)
Sn2−O236	2.091(5)	Sn2−O234′	2.023(5)	Sn5−O135′	2.116(5)
Sn3−O134′	2.102(5)	Sn3−O135′	2.026(5)	Sn6−O126	2.113(5)
Sn3−O234′	2.065(5)	Sn3−O236	2.023(5)	Sn6−O236	2.123(5)
⟨**Sn$_h$**−**O**⟩	2.080	⟨**Sn$_h$**−**OH**⟩	2.120	⟨**Sn$_p$**−**C**⟩	2.121
Sn4−O456	2.087(5)	Sn4−O46	2.127(5)	Sn1−C10	2.135(9)
Sn5−O456	2.082(5)	Sn4−O45	2.111(5)	Sn2−C20	2.100(8)
Sn6−O456	2.071(5)	Sn5−O45	2.113(5)	Sn3−C30	2.127(8)
⟨**O**−**H**···**O**⟩	2.74	Sn5−O56	2.116(6)	⟨**Sn$_h$**−**C**⟩	2.128
O45−O45X	2.805(9)	Sn6−O46	2.116(5)	Sn4−C40	2.122(9)
O46−O46X″	2.707(9)	Sn6−O56	2.132(5)	Sn5−C50	2.136(8)
O56−O56X″	2.71(1)			Sn6−C60	2.127(8)
⟨**Sn$_p$**···**Sn$_p$**⟩	3.208	⟨**Sn$_p$**···**Sn$_h$**⟩	3.826	⟨**Sn$_h$**···**Sn$_h$**⟩	3.294
Sn1−Sn2	3.2208(8)	Sn1−Sn4	3.8085(8)	Sn4−Sn5	3.2875(8)
Sn1−Sn3′	3.2132(8)	Sn1−Sn6	3.8029(8)	Sn4−Sn6	3.2969(8)
Sn2−Sn3	3.1915(8)	Sn2−Sn4′	3.8323(8)	Sn5−Sn6	3.2980(8)
⟨**Sn$_p$**···**Sn$_h$**⟩	3.294	Sn2−Sn5′	3.8385(8)	⟨**Sn$_p$**···**O$_{diox}$**⟩	3.30
Sn1−Sn5′	3.2757(8)	Sn3−Sn5	3.8436(8)	Sn2−O1	3.244(6)
Sn2−Sn6	3.3049(8)	Sn3−Sn6	3.8307(8)	Sn3−O1	3.356(6)
Sn3−Sn4′	3.3027(8)			⟨**S**−**O**⟩	1.449
		S1−C70	1.761(9)	S1−O45X	1.437(7)
		O1−C1A	1.44(1)	S1−O46X	1.454(8)
		O1−C1B	1.42(1)	S1−O56X	1.455(8)

⟨**O**−**Sn$_h$**−**OH**⟩$_c$	91.2	⟨**O**−**Sn$_h$**−**OH**⟩$_c$	76.4	⟨**O**−**Sn$_p$**−**C**⟩$_c$	111.1	⟨**HO**−**Sn$_h$**−**C**⟩$_c$	97.8
O134−Sn4−O46	90.9(2)	O456−Sn4−O46	76.1(2)	O125−Sn1−C10	109.5(3)	O46−Sn4−C40	96.8(3)
O234−Sn4−O45	92.2(2)	O456−Sn4−O45	76.5(2)	O135−Sn1−C10	109.4(3)	O45−Sn4−C40	96.6(3)
O125′-Sn5-O45	92.2(2)	O456−Sn5−O45	76.6(2)	O134−Sn1−C10	112.0(3)	O45−Sn5−C50	98.0(3)
O135′-Sn5-O56	90.2(2)	O456−Sn5−O56	76.4(2)	O126−Sn1−C10	111.6(3)	O56−Sn5−C50	99.2(2)
O126−Sn6−O46	91.3(2)	O456−Sn6−O46	76.7(2)	O125−Sn2−C20	104.3(3)	O46−Sn6−C60	99.1(3)
O236−Sn6−O56	90.7(2)	O456−Sn6−O56	76.3(2)	O126−Sn2−C20	105.9(3)	O56−Sn6−C60	97.2(3)
⟨**O**−**Sn$_h$**−**O**⟩$_c$	76.1	⟨**HO**−**Sn$_h$**−**OH**⟩$_c$	96.4	O236−Sn2−C20	118.8(3)	⟨**O**−**Sn$_h$**−**C**⟩$_c$	99.1
O134−Sn4−O234	75.6(2)	O46−Sn4−O45	96.3(2)	O234′-Sn2-C20	118.8(3)	O134−Sn4−C40	100.6(3)
O125′-Sn5-O135′	76.5(2)	O45−Sn5−O56	96.0(2)	O135′-Sn3-C30	105.7(3)	O234−Sn4−C40	100.4(3)
O126−Sn6−O236	76.1(2)	O46−Sn6−O56	97.0(2)	O134′-Sn3-C30	106.8(3)	O125′-Sn5-C50	98.0(3)
⟨**O**−**Sn$_h$**−**O**⟩$_c$	87.7	⟨**O**−**Sn$_h$**−**OH**⟩$_t$	160.2	O236−Sn3−C30	116.9(3)	O135′-Sn5-C50	99.0(3)
O134−Sn4−O456	87.6(2)	O234−Sn4−O46	159.7(2)	O234′-Sn3-C30	116.9(3)	O126−Sn6−C60	99.4(3)
O234−Sn4−O456	88.1(2)	O134−Sn4−O45	160.4(2)			O236−Sn6−C60	97.4(2)
O125′-Sn5-O456	87.5(2)	O135′-Sn5-O45	160.7(2)	⟨**O**−**Sn$_h$**−**C**⟩$_t$	171.1	⟨**Sn$_p$**−**O**−**Sn$_p$**⟩	102.5
O135′-Sn5-O456	87.2(2)	O125′-Sn5-O56	159.7(2)	O456−Sn4−C40	169.3(3)	Sn1−O125−Sn2	103.1(2)
O126−Sn6−O456	88.0(2)	O126−Sn6−O56	159.9(2)	O456−Sn5−C50	172.5(3)	Sn1−O135−Sn3′	102.5(2)
O236−Sn6−O456	88.1(2)	O236−Sn6−O46	160.8(2)	O456−Sn6−C60	171.6(3)	Sn1−O134−Sn3′	102.4(2)
⟨**O**−**Sn$_p$**−**O**⟩$_c$[b]	77.4	⟨**O**−**Sn$_p$**−**O**⟩$_c$	96.7			Sn1−O126−Sn2	102.6(2)
O125−Sn1−O135	77.5(2)	O134−Sn1−O126	98.1(2)			Sn2−O236−Sn3	101.7(2)
O135−Sn1−O134	77.6(2)	O125−Sn2−O234′	96.0(2)			Sn2′−O234−Sn3′	102.6(2)
O125−Sn1−O126	77.6(2)	O135′-Sn3-O236	95.9(2)	⟨**Sn$_p$**−**O**−**Sn$_h$**⟩	103.2	⟨**Sn$_p$**−**O**−**Sn$_h$**⟩	135.0
O125−Sn2−O126	76.6(2)	⟨**O**−**Sn$_p$**−**O**⟩$_t$	135.6	Sn1−O125−Sn5′	103.1(2)	Sn2−O125−Sn5′	136.0(3)
O126−Sn2−O236	77.1(2)	O135−Sn1−O126	137.2(2)	Sn1−O135−Sn5′	102.2(2)	Sn3′−O135−Sn5′	136.2(3)
O236−Sn2−O234′	77.4(2)	O125−Sn1−O134	136.7(2)	Sn3′−O134−Sn4	103.1(2)	Sn1−O134−Sn4	134.1(3)
O135′-Sn3-O134′	77.2(2)	O125−Sn2−O236	134.1(2)	Sn2−O126−Sn6	103.4(2)	Sn1−O126−Sn6	133.5(3)
O134′-Sn3-O234′	77.2(2)	O126−Sn2−O234′	135.0(2)	Sn2−O236−Sn6	103.3(2)	Sn3−O236−Sn6	135.0(2)
O236−Sn3−O234′	78.1(2)	O134′-Sn3-O236	135.9(2)	Sn3′−O234−Sn4	104.0(2)	Sn2′−O234−Sn4	135.0(3)
		O135′-Sn3-O234′	135.0(2)	⟨**Sn$_h$**−**O**−**Sn$_h$**⟩	104.7	⟨**Sn$_h$**−**OH**−**Sn$_h$**⟩	102.0
				Sn4−O456 −Sn6	104.9(2)	Sn4−O46 −Sn6	102.0(2)
				Sn4−O456−Sn5	104.1(2)	Sn4−O45−Sn5	102.2(2)
				Sn5−O456 −Sn6	105.1(2)	Sn5−O56−Sn6	101.9(2)
				⟨**O**−**S**−**O**⟩	113.0	⟨**O**−**S**−**C**⟩	105.6
				O45X−S1−O46X	111.1(5)	O45X−S1−C70	106.1(4)
				O45X−S1−O56X	113.9(1)	O46X−S1−C70	104.9(5)
				O46X−S1−O56X	114.0(4)	O56X−S1−C70	105.9(5)

[a] Legend: subscripts p and h refer to five and six-coordinate tin atoms, respectively; ′ refers to the symmetry $-x, -y, -z$; ″ refers to the symmetry $1 - x, -y, -z$; subscripts c and t refer to cis and trans positions, respectively. [b] Bond distances and angles in broken brackets denote average values.

This loss of dioxane upon aging appears unavoidable. After the first weight loss, the compound, stable up to 250 °C, is identified as **1**, $\{(BuSn)_{12}O_{14}(OH)_6\}(4\text{-}CH_3C_6H_4SO_3)_2$, by ^{119}Sn NMR (vide infra) and elemental analyses. The three subsequent weight losses (∼290 °C, strongly exothermic; ∼400 °C, strongly exothermic; between 600 and 900 °C, weakly exothermic) cannot be assigned. The one around 290 °C likely involves combustion of butyl chains, since BuSnO(OH)[13] and other $\{(BuSn)_{12}O_{14}(OH)_6\}X_2$ compounds ($X = OH^-$, OAc^-) decompose around the same temperature.

Solid-State ^{119}Sn MAS NMR Studies of 1·diox and 1. Figure 4 presents the ^{119}Sn MAS NMR spectra

(13) Blunden, S. J.; Hill, R.; Suton, S. E. *Appl. Organomet. Chem.* **1991**, *5*, 159.

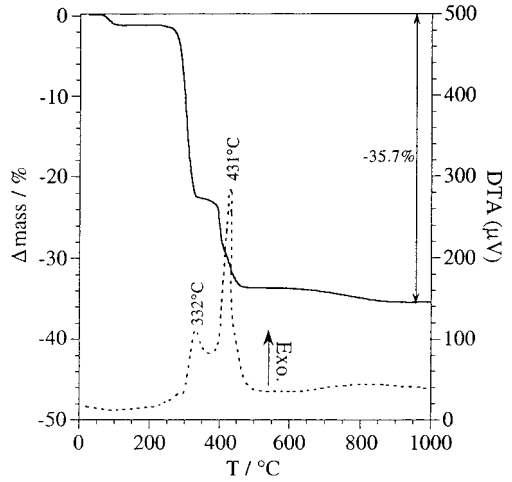

Figure 3. Simultaneous thermogravimetric (TGA) and differential thermal (DTA) analyses of $\{(BuSn)_{12}O_{14}(OH)_6\}(4\text{-}CH_3C_6H_4SO_3)_2\cdot C_4H_8O_2$ (**1**·diox) at 10 °C/min and under pure oxygen.

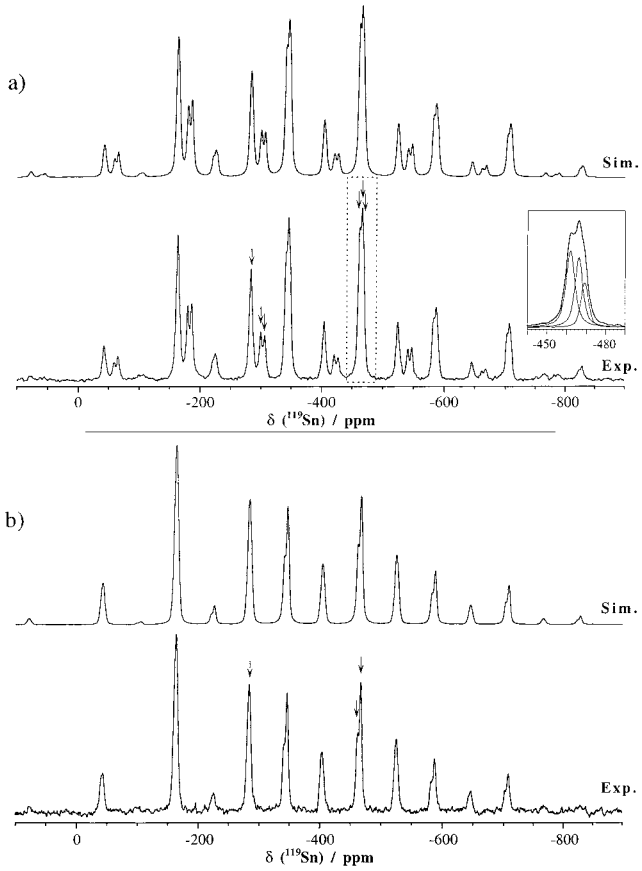

Figure 4. Experimental and simulated ^{119}Sn MAS NMR spectra of (a) $\{(BuSn)_{12}O_{14}(OH)_6\}(4\text{-}CH_3C_6H_4SO_3)_2\cdot C_4H_8O_2$ (**1**·diox) and (b) $\{(BuSn)_{12}O_{14}(OH)_6\}(4\text{-}CH_3C_6H_4SO_3)_2$ (**1**). $\nu_{MAS} = 13.5$ kHz, and isotropic resonances are pointed with arrows. In (a) the insert shows an expansion of the isotropic resonances of the six-coordinate tin atoms.

of **1**·diox and **1**. For both compounds, the isotropic chemical shifts around −300 and −460 ppm are easily assigned to five- and six-coordinate tin atoms, respectively. The spectra were simulated in order to quantify each site. Results are gathered in Table 2.

For **1**·diox, the number of isotropic resonances, three for each coordination type, is in agreement with the number of nonequivalent tin atoms in the X-ray structure. However, the quantification inside each coordination does not agree with the structure. This discrepancy likely arises from a partial loss of dioxane, as for TGA, which results in a sample made of a mixture of **1**·diox and **1**. Therefore, a precise assignment of the ^{119}Sn NMR resonances and the determination of the principal components of the ^{119}Sn shielding tensors[14−16] are not possible, except for the more shielded and equally populated five-coordinate sites (B and C), which can be assigned to Sn2 and Sn3. Indeed, they have additional remote contacts with a dioxane oxygen and therefore belong only to **1**·diox. The latter assignment is confirmed by the disappearance of the low-frequency resonances upon removing dioxane. A further assignment (Sn3 = B and Sn2 = C), based on the Sn−O1 distances, would be too speculative.

Table 2. ^{119}Sn MAS NMR Data[a]

signal	δ_{iso}, ppm	ζ, ppm	η	σ_{11}, ppm	σ_{22}, ppm	σ_{33}, ppm	intens[b]	coord
$\{(BuSn)_{12}O_{14}(OH)_6\}(4\text{-}CH_3C_6H_4SO_3)_2\cdot C_4H_8O_2$ (**1**·diox)								
A	−283.9						3.4	5
B	−300.3	398.2	0.20	62.3	141.0	698.6	1.4	5 + 1
C	−306.9	434.4	0.25	35.4	144.0	741.3	1.3	5 + 1
D	−462.0						2.5	6
E	−466.3						2.2	6
F	−469.3						1.3	6
$\{(BuSn)_{12}O_{14}(OH)_6\}(4\text{-}CH_3C_6H_4SO_3)_2$ (**1**)								
X	−283.9	386.2	0.20	52.2	129.4	670.1	6.7	5
Y	−461.7	313.8	0.30	257.7	351.9	775.5	1.9	6
Z	−467.4	325.8	0.30	255.6	353.4	793.2	3.4	6

[a] $\delta_{iso} = -\sigma_{iso} = -(\sigma_{11} + \sigma_{22} + \sigma_{33})/3$, $\zeta = \sigma_{33} - \sigma_{iso}$, and $\eta = |\sigma_{22} - \sigma_{11}|/|\sigma_{33} - \sigma_{iso}|$, where σ_{11}, σ_{22}, and σ_{33} are the principal components of the ^{119}Sn shielding tensor, ordered with the following rule: $|\sigma_{33} - \sigma_{iso}| \geq |\sigma_{11} - \sigma_{iso}| \geq |\sigma_{22} - \sigma_{iso}|$. [b] Intensities have been normalized to 12 for each compound.

The ^{119}Sn MAS NMR spectrum of **1** (Figure 4b) reveals only a single ^{119}Sn signal for all six five-coordinate tin atoms and two signals (−461.7 and −467.4 ppm), roughly in a 2:4 ratio, for the six-coordinate ones. This apparent C_{2v} symmetry, upon removing dioxane, is in line with the conservation of the structure of $\{(BuSn)_{12}O_{14}(OH)_6\}(PTS)_2$ and results from two sulfonate oxygens being close to Sn6 and a single oxygen from another sulfonate unit being close to Sn4 and Sn5. This allows a tentative assignment of site Y (−461.7 ppm) to Sn6. The principal components of the ^{119}Sn shielding tensors[14−16] of **1** are reported in Table 2.

Solution NMR Studies of 1·diox and 1. The solution ^{119}Sn{^{1}H} NMR spectra of **1**·diox and **1** in CD_2Cl_2 are identical and are similar to spectra previously reported for other $\{(BuSn)_{12}O_{14}(OH)_6\}^{2+}$-based compounds.[8,9,17,18] They consist of two concentration-independent, sharp ^{119}Sn resonances at −282.8 and −461.8 ppm, respectively assigned to the five- and six-coordinate tin atoms. Each resonance is flanked by three sets of $^2J(^{119}Sn-O-^{119/117}Sn)$ satellites, corresponding to a

(14) Klaus, E.; Sebald, A. *Magn. Reson. Chem.* **1994**, *32*, 679.
(15) Harris, R. K.; Lawrence, S. E.; Oh, S. W. *J. Mol. Struct.* **1995**, *347*, 309.
(16) Ribot, F.; Sanchez, C.; Meddour, A.; Gielen, M.; Tiekink, E. R. T.; Biesemans, M.; Willem, R. *J. Organomet. Chem.* **1998**, *552*, 177.
(17) Ribot, F.; Sanchez, C.; Willem, R.; Martins, J. C.; Biesemans, M. *Inorg. Chem.* **1998**, *37*, 911.
(18) Ribot, F.; Banse, F.; Diter, F.; Sanchez, C. *New J. Chem.* **1995**, *19*, 1145.

Table 3. Solution NMR Data for $\{(BuSn)_{12}O_{14}(OH)_6\}(4\text{-}CH_3C_6H_4SO_3)_2\cdot C_4H_8O_2$ (1·diox) in CD_2Cl_2[a,b]

$\delta(^1H)$, ppm	$^nJ(^1H-^{119}Sn)$[g], Hz	$\delta(^{13}C)$, ppm	$^nJ(^{13}C-^{119/117}Sn)$, Hz	assignt
1.66 (t)[h]	101	21.7	860/820	$Sn_pCH_2CH_2CH_2CH_3$
1.27 (t)[h]	126	27.2	1162/1114	$Sn_hCH_2CH_2CH_2CH_3$
1.79 (quint)[h]	160	27.0	51[i]	$Sn_pCH_2CH_2CH_2CH_3$
1.63 (quint)[h]	125	28.0	54[i]	$Sn_hCH_2CH_2CH_2CH_3$
1.52 (sext)[h]		26.2	92[i]	$Sn_pCH_2CH_2CH_2CH_3$
1.38 (sext)[h]		26.5	163/155	$Sn_hCH_2CH_2CH_2CH_3$
0.97 (t)[h]		13.5		$Sn_pCH_2CH_2CH_2CH_3$
0.91 (t)[h]		13.8		$Sn_hCH_2CH_2CH_2CH_3$
7.02 (s)[h]	1.05[j]			μ_2-OH
		140.6		ipso $O_3SC_6H_4CH_3$
7.69 (d)[h]		126.0		ortho $O_3SC_6H_4CH_3$
7.20 (d)[h]		128.3		meta $O_3SC_6H_4CH_3$
		141.7		para $O_3SC_6H_4CH_3$
2.37 (s)[h]		21.2		$O_3SC_6H_4CH_3$
3.65 (s)[h]		67.2		$C_4H_8O_2$

[a] Chemical shifts referenced as in the Experimental Section. $\delta(Sn_p)$ −282.8 ppm [423/405,[c] 162,[d] 42[e]]; $\delta(Sn_h)$ −461.8 ppm [423/405,[c] 176,[f] 42[e]]. [b] In solutions of ca. 50 mg of substance per 0.5 mL of solvent. [c] $^2J(^{119}Sn_p-^{119/117}Sn_h)$ or $^2J(^{119}Sn_h-^{119/117}Sn_p)$ coupling constant in Hz (single oxo bridge). [d] $^2J(^{119}Sn_p-^{117}Sn_p)$ coupling constant in Hz (double oxo bridge). [e] Unresolved $^2J(^{119}Sn_p-^{119/117}Sn_h)$ or $^2J(^{119}Sn_h-^{119/117}Sn_p)$ coupling constant in Hz (double oxo bridge). [f] $^2J(^{119}Sn_h-^{117}Sn_h)$ coupling constant in Hz (double oxo−hydroxo bridge). [g] $^nJ(^1H-^{119}Sn)$ coupling constants, as determined from cross sections of the 2D $^1H-^{119}Sn$ HMQC spectrum. [h] Multiplicity due to $^nJ(^1H-^1H)$. [i] Unresolved $^nJ(^{13}C-^{119/117}Sn)$. [j] Measured through $^1H-^{119}Sn$ *J*-HMQC technique.

total of four different types of connectivity paths existing between two tin atoms in $\{(BuSn)_{12}O_{14}(OH)_6\}^{2+}$, in agreement with previous data.[9] The ^{119}Sn as well as the ^1H and ^{13}C NMR data are reported in Table 3.

The assignment of the butyl proton resonances to their respective five- or six-coordinate tin atoms was achieved by gradient-enhanced $^1H-^{119}Sn$ correlation NMR spectroscopy, as described previously.[17,19] Further assignments were performed by comparison with reported data and, in the case of ^{13}C, also on the basis of $^nJ(^{13}C-^{119/117}Sn)$ coupling constants.[9,17]

The identical solution ^{119}Sn NMR spectra of **1**·diox and **1**, as well as the very good agreement between the solution chemical shifts and the solid-state isotropic shifts for **1**, indicate that the Lewis interaction between five-coordinate tin atoms and dioxane in the solid state is completely lost when **1**·diox is dissolved. This inteaction is therefore fairly weak in the solid state (even if it is detectable by ^{119}Sn MAS NMR) and is likely only due to packing. The weakness of this interaction is stressed by the ^{119}Sn NMR chemical shifts of compound **1** in pure dioxane (diox/Sn = 12) which display no significant effect for both coordinations. A Lewis interaction between five-coordinate tin atoms and DMSO is reported for $\{(BuSn)_{12}O_{14}(OH)_6\}(O_2PPh_2)_2$ in CD_2Cl_2/DMSO (1/1 v/v), the ^{119}Sn chemical shift of the five-coordinate tin atoms being low-frequency-shifted by 25 ppm.[17] In contrast, compound **1** does not interact significantly with DMSO, since its concentration-independent ^{119}Sn chemical shift for five-coordinate tin at −285.4 ppm remains unchanged. Thus, the affinity of five-coordinate tin for Lewis bases in the $\{(BuSn)_{12}O_{14}(OH)_6\}^{2+}$ macrocation depends on the nature of the counteranion.

The absence of ionic dissociation for $\{(BuSn)_{12}O_{14}(OH)_6\}X_2$ compounds in low dielectric constant solvents, such as CD_2Cl_2 (ϵ = 8.9), has been recently evidenced for $\{(BuSn)_{12}O_{14}(OH)_6\}(O_2PPh_2)_2$.[17] For compound **1**, the strong contact between the cage poles and the sulfonate anions still holds, as evidenced by the similarity of the CD_2Cl_2 solution- and solid-state isotropic ^{119}Sn chemical shifts, especially for the six-coordinate tin atoms. Nuclear Overhauser effect spectroscopy (NOESY)[20] and rotating-frame nuclear Overhauser effect spectroscopy (ROESY)[21] experiments have been performed in order to evaluate the distance between the macrocation and the counteranion as a function of the solvent. In the 2D ROESY experiment, cross-peaks were detected between proton resonances of the macrocation (μ_2-OH, α-, *β*-, and *γ*-CH_2, and CH_3 of the butyl chains of the six-coordinate tin atoms) and the ortho proton resonances of the PTS^- anion, which unambiguously proves their close proximity. Less relevant cross-peaks within the macrocation and within the PTS^- anion were also observed. In 2D NOESY spectra (303 K), comparison of the signs of cross-peaks and diagonal peaks revealed the same slow rotational tumbling regime for the μ_2-OH and the PTS^- protons but a fast one for those of the butyl chains (probably because of their conformational freedom).[20,21] Therefore, the distance separating the ortho PTS and the μ_2-OH protons is the only one for which a determination, using cross-peak volumes derived from three ROESY experiments, is relevant (see Experimental Section). This distance was estimated at 3.8 ± 0.1 Å, taking the ortho−meta proton distance (2.48 Å)[22] as an internal reference. Globally, the main conclusion is that, in CD_2Cl_2, a medium with low dielectric constant, the *p*-toluenesulfonate anions remain in close contact with the "poles" of the macrocation.

The ionic conductivity of **1** in CD_2Cl_2 was identical with that of the pure solvent (ca. 5 $\mu S\ cm^{-1}$), confirming the absence of ionic dissociation. However, the bridging mode between the macrocation and the sulfonates in the solid state is most probably not maintained in solution. Therefore, when **1** or **1**·diox is dissolved in CD_2Cl_2, each

(19) Willem, R.; Bouhdid, A.; Kayser, F.; Delmotte, A.; Gielen, M.; Martins, J. C.; Biesemans, M.; Tiekink, E. R. T., *Organometallics* **1996**, *15*, 1920.

(20) (a) Neuhaus, D.; Williamson, M. P. *The Nuclear Overhauser Effect in Structural and Conformational Analysis*; VCH: New York, 1989. (b) Cavanagh, J.; Fairbrother, W. J.; Palmer, A. G., III; Skelton, N. J. *Protein NMR Spectroscopy Principles and Practice*; Academic Press: San Diego, CA, 1996.

(21) (a) Bothner-By, A. A.; Stephens, R. L.; Lee, J.-M.; Warren, C. D.; Jeanloz, R. W. *J. Am. Chem. Soc.* **1984**, *106*, 811. (b) Bax, A.; Davis, D. G. *J. Magn. Reson.* **1985**, *63*, 207.

(22) The ortho−meta H−H distance was determined from a phenyl moiety available in the Insight II builder fragment library (Insight II, 95.0, MSI Scranton Road, San Diego, CA).

sulfonate likely switches to a "terminal" position, with its S−C bond along the macrocation 3-fold axis (passing through O456 and its symmetric counterpart) and its three oxygen atoms being hydrogen-bonded to the three hydroxy groups of a single cage pole. This arrangement does not break the D_{3d} symmetry observed in solution on the ^{119}Sn NMR time scale, if it is reasonably assumed that the aromatic ring freely rotates around the S−C axis. This proposal is supported by the ^{119}Sn chemical shift of −461.8 ppm, which is nearly identical with the isotropic chemical shift of site Y, assigned to Sn6, a six-coordinate tin for which both hydroxy groups are hydrogen-bonded to the same sulfonate moiety (vide supra). Setting the distance between the protons of the bridging hydroxy group and the ortho protons of PTS^- to 3.8 Å (ROESY experiment) results in the distance between the oxygen of a bridging hydroxy group and the oxygen of the sulfonate, which faces it, to be 2.5 Å, in satisfactory agreement with the typical distance separating two oxygen atoms in a strong hydrogen bond.[23]

In DMSO-d_6, the chemical shift of the six-coordinate ^{119}Sn resonances moves to −473.5 ppm, for any concentration from 2×10^{-3} to 2×10^{-1} mol/L. A similar low-frequency shift was already observed for $\{(BuSn)_{12}O_{14}(OH)_6\}(O_2PPh_2)_2$ in CD_2Cl_2/DMSO (1/1 v/v) and correlated to an increase of the distance separating the cage poles from the anions in a more polar medium.[17] Indeed, 2D ^{1}H−^{1}H NOESY experiments in DMSO-d_6 at 303 K reveal positive cross-peaks between the μ_2-OH and all the butyl protons but negative cross-peaks between the protons within the anion PTS^- and no cross-peak at all between the μ_2-OH and the ortho aromatic protons of PTS^-. This observation demonstrates that the anion is tumbling faster than the macrocation and, therefore, no longer has any tight contact with it. Moreover, the absence of a cross-peak between the cluster and anion protons also points to full cation−anion dissociation. In DMSO-d_6, which has a higher viscosity than CD_2Cl_2, the butyl chains appear to be less mobile. Control ROESY experiments all miss the cross-peak between the μ_2-OH and the ortho aromatic protons of PTS^-, which proves that the lack of cross-peak in the NOESY spectra is not due to an unfortunate correlation time and strengthens the view of full cation−anion dissociation in DMSO ($\epsilon = 46.7$).

The conductivity values for **1** in DMSO range from 200 to 1210 μS cm^{-1} (pure solvent: 5.5 μS cm^{-1}) for concentrations of 5×10^{-3} to 5×10^{-2} mol/L, respectively, in complete agreement with the cation−anion dissociation proposed above.

For the first time for such $\{(BuSn)_{12}O_{14}(OH)_6\}^{2+}$ macrocations, the proton resonance around 7 ppm (7.02 ppm in CD_2Cl_2 and 7.33 ppm in DMSO-d_6) displayed a ^{1}H−^{119}Sn HMQC correlation with the ^{119}Sn resonance of the six-coordinate tin atoms, none being observed for the five-coordinate ones. This assigns this proton resonance to the cage pole bridging μ_2-OH hydroxy groups.

The $^2J(^1H-O-^{119}Sn_h)$ coupling constant between the μ_2-OH hydroxy proton and the six-coordinate ^{119}Sn nuclei was determined by the *J*-HMQC technique.[24] This technique which, to the best of our knowledge, has not been described so far for ^{1}H−^{119}Sn correlations, is particularly suited for the determination of weak coupling constants between protons and low abundant spin $^1/_2$ nuclei when the coupling satellites are unresolved in the standard or HMQC spectra (see Experimental Section).[24,25]

The value found for this coupling constant is strongly dependent on the solvent: 1.05 ± 0.04 Hz in CD_2Cl_2 and 4.01 ± 0.05 Hz in DMSO-d_6. This observation is again in line with the fact that the μ_2-OH groups are involved in H-bridge interactions with the counteranion in CD_2Cl_2 solution. This should be associated with weakening of the O−H bond and, accordingly, result in a small $^2J(^1H-O-^{119}Sn_h)$ scalar coupling between this OH and the six-coordinate ^{119}Sn nucleus, as observed. In contrast, in DMSO-d_6, where such an interaction is no longer present, the $^2J(^1H-O-^{119}Sn_h)$ scalar coupling is considerably larger and is apparently representative of $^2J(^1H-O-^{119}Sn_h)$ couplings of μ_2-OH hydroxy bridges bound to tin without H-bond interactions toward charged species such as the PTS^- anion.[19] However, this does not exclude weaker H-bonds with DMSO.

Study of the Reaction between BuSnO(OH) and HPTS. Reaction conditions were varied, and attention was paid to the starting sulfur-to-tin ratio (S/Sn = 2/12, 2.5/12, 3/12, 3.5/12, 4/12, 8/12), the solvent which controls the reflux temperature (cyclohexane, toluene, or xylene), and the reflux time (from 1 to 48 h). The main results are given in Table 4. Except for the starting ratio S/Sn = 8/12 (for which some additional unidentified broad and weak resonances were observed (−295, −481, and −487 ppm)), the ^{119}Sn NMR fingerprint of $\{(BuSn)_{12}O_{14}(OH)_6\}(PTS)_2$ (**1**; −282.8 and −461.8 ppm) constituted apparently the only identifiable set of signals for the crude products. However, the integration curves (Figure 5) reveal the presence of a hidden signal in the noise at the low-frequency side of the six-coordinate ^{119}Sn resonance. This arises probably from ill-defined butyltin oxo polymeric species that are soluble in the same organic solvents as compound **1** (i.e., benzene, toluene, cyclohexane, xylene, dichloromethane, chloroform, THF, DMSO, 1,4-dioxane, DMF). Their very broad signals in solution ^{119}Sn NMR likely result from too long rotational correlation times related to their polymeric nature.

Solid-state MAS NMR with a Hahn echo provided more direct evidence. Figure 6 compares experimental and simulated ^{119}Sn NMR MAS spectra obtained with

(23) The solution structural model was constructed as follows. The macrocation was built with a D_{3d} symmetry using the averaged distances and angles of the X-ray structure (Table 1). The hydrogen atoms of the μ_2-OH groups were placed with the following conditions: d(O−H) = 1.00 Å and the O−H bond parallel to the 3-fold axis. The sulfonate group of PTS^- was also built using the averages of the X-ray structure (Table 1), while its benzene ring was set to an ideal geometry; i.e., d(C−C) = 1.39 Å, d(C−H) = 1.09 Å, ∠(C−C−C) = 120°, and ∠(C−C−H) = 120°. PTS^- was aligned on the 3-fold axis of the cluster, its oxygen atoms facing the μ_2-OH groups. The location of PTS^- relative to the macrocation was fixed according to the distance between the ortho protons of the PTS^- and the protons of the μ_2-OH group, determined to be 3.8 Å by NMR experiments. To take into account the free rotation of the benzene ring along the S−C bond (aligned on the 3-fold axis), this distance was considered as the distance between two planes, both perpendicular to the 3-fold axis, the first one passing through the ortho protons and the second one through the protons of the μ_2-OH. This model fully defines a possible geometry for the cation−anion interaction and allows the distance $d(O_{cation}-O_{anion})$ to be calculated at 2.5 Å.

(24) Willker, W.; Leibfritz, D. *Magn. Reson. Chem.* **1995**, *33*, 632.
(25) Martins, J. C.; Biesemans, M.; Willem, R. *Prog. NMR Spectrosc.*, in press.

Table 4. Experimental Conditions and Selected Data for the Reaction of BuSnO(OH) with *p*-Toluenesulfonic Acid

exptl conditions			mass of crude	chem anal. of crude prod.[c]		% compd **1** in crude prod.	
HPTS/12 Sn	solv[a]	time, h	product,[b] mg	Sn, %	S/12 Sn	cryst[d]	RMN[e]
2.0	T	48	18.4	51.8	1.46	11	40
2.5	T	48	20.3	51.7	1.51	xxx[f]	50
3.0	T	48	21.8	48.1	2.50.	60	60
3.5	T	48	20.8	49.4	2.26	55	55
4.0	T	48	22.6	47.9	3.10	50	50
8.0	T	48	21.9	39.9	6.66	0	~5
4.0	T	1	25.2	46.5	3.02	xxx	50
4.0	T	6	23.3	46.7	3.43	xxx	50
4.0	T	24	23.7	46.8	3.57	xxx	50
4.0	C	48	20.6	nd[g]	nd	xxx	65
4.0	X	48	23.9	nd	nd	xxx	65

[a] Legend: T, toluene (bp 111 °C); C, cyclohexane (bp 81 °C); X, xylene (bp 140 °C). [b] Soluble product obtained after reaction and recovered by filtration and evaporation under reduced pressure (see Experimental Section). [c] For $\{(BuSn)_{12}O_{14}(OH)_6\}(PTS)_2$: Sn, 51.3% and S/12 Sn = 2. [d] From the yield obtained by crystallization in dioxane and subsequent drying (see Experimental Section), ±2%. [e] From quantitative ^{119}Sn NMR (see Experimental Section), ±5%. [f] "xxx" indicates that the crystallization step did not proceed correctly. Visually, millimetric crystals (**1**·diox) were mixed with a fine powder. Global elemental analyses for such precipitates were incompatible with the only presence of compound **1** (S/Sn ≠ 2/12). [g] nd = not determined.

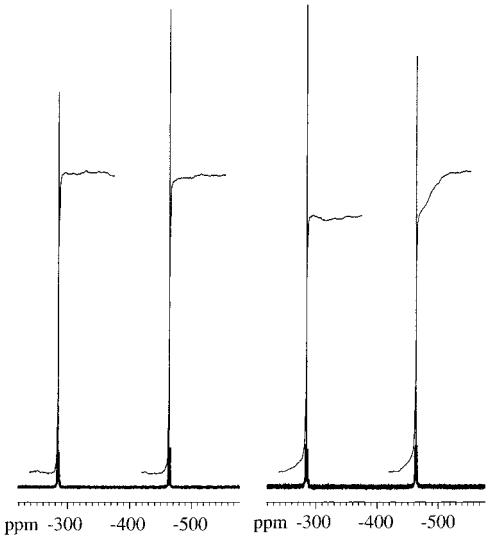

Figure 5. Experimental integration curves in the solution (CD_2Cl_2) ^{119}Sn{^{1}H} NMR spectra of $\{(BuSn)_{12}O_{14}(OH)_6\}$-(4-$CH_3C_6H_4SO_3)_2$ (**1**; left panel) and of a crude reaction product (right panel) corresponding to S/Sn = 3/12, 48 h, toluene. Integrals are only comparable within each of the spectra.

a Hahn echo for compound **1** and a crude product (S/Sn = 3/12, 48 h, toluene). For compound **1**, the results are, as expected, identical within experimental error to those presented in Table 2 for a standard ^{119}Sn MAS experiment. For the crude product, the solid-state ^{119}Sn NMR fingerprint of compound **1** is again observed (sites 1−3 of Figure 6 corresponding, respectively, to sites X−Z of Table 2), but one additional, extremely broad, anisotropy pattern (site 4 in Figure 6) can now also be deconvoluted and accounts for roughly 35% of tin nuclei. This amount matches satisfactorily the one missing in quantitative solution ^{119}Sn NMR. The 10-fold broader lines of site 4 were never visible in a standard MAS experiment, where they are lost in the dead time because of their rapid decay.[26] Site 4 is attributed to the ill-defined additional species.

(26) (a) Massiot, D.; Farnan, I.; Gautier, N.; Trumeau, D.; Trokiner, A.; Coutures, J.-P. *Solid State NMR* **1995**, *4*, 241. (b) Fayon, F.; Bessada, C.; Massiot, D.; Farnan, I.; Coutures, J.-P. *J. Non-Cryst. Solids* **1998**, *232−234*, 403.

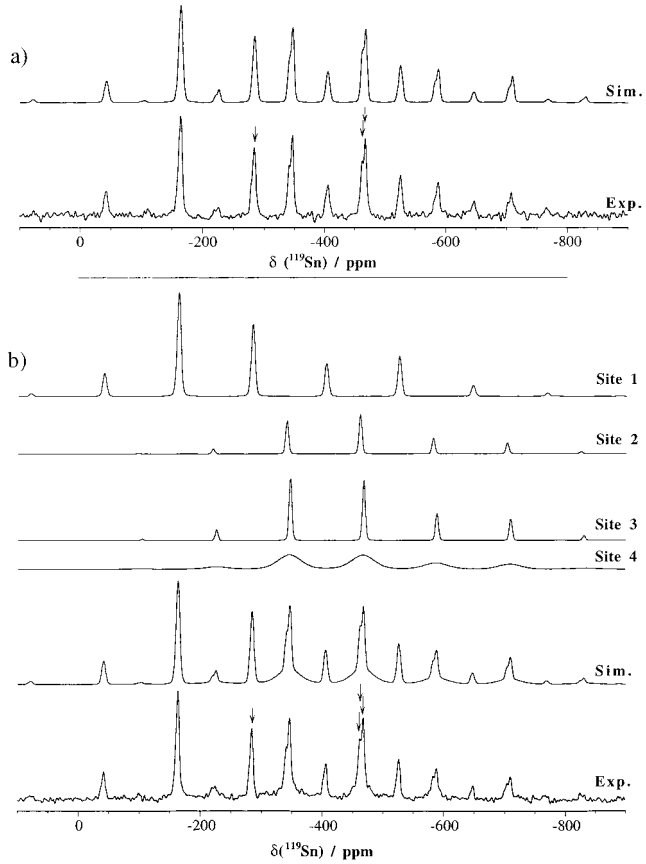

Figure 6. Experimental and simulated ^{119}Sn MAS NMR spectra obtained with a rotor-synchronized Hahn echo for (a) $\{(BuSn)_{12}O_{14}(OH)_6\}$(4-$CH_3C_6H_4SO_3)_2$ (**1**) and for a crude reaction product (b) corresponding to S/Sn = 3/12, 48 h, toluene. ν_{MAS} = 13.5 kHz, τ = 74 μs, and isotropic resonances are denoted with arrows.

Quantitative solution ^{119}Sn NMR (Table 4) enabled us to optimize the reaction conditions. Substituting toluene (bp 110.6 °C) for cyclohexane (bp 80.7 °C) or xylene (bp 140 °C) gave a larger proportion of compound **1** in the crude materials (65% against 50% in toluene), but crystallization could not eliminate byproducts. Increasing the refluxing time from 1 to 48 h did not change the percentage of **1** in the crude product (ca. 50%) but was needed for correct crystallization. The best

yield in pure crystallized compound **1**·diox (60%) was obtained from a starting S/Sn ratio of 3/12, with toluene refluxing for 48 h.

Experimental Section

Syntheses. Butyltin hydroxide oxide, BuSnO(OH) (Aldrich or Strem Chemicals), and *p*-toluenesulfonic acid monohydrate, HPTS·H_2O (Fluka), were used as received. The reactions were performed in a 1 L round-bottom flask equipped with a Dean−Stark apparatus water trap and a condenser. For each experiment, 20 g of BuSnO(OH) and the appropriate amount of HPTS·H_2O for various starting S/Sn ratios (2/12, 2.5/12, 3/12, 3.5/12, 4/12, or 8/12) were suspended in 500 mL of solvent (cyclohexane, toluene, or xylene) and refluxed for 1−48 h, during which time water was trapped in the Dean−Stark apparatus. Subsequently, the reaction mixture was cooled and filtered on a fritted glass (No. 4). The clear solutions obtained were evaporated under reduced pressure to yield a white amorphous crude solid. In contrast to the starting materials, BuSnO(OH) and HPTS·H_2O, all crude products are quite soluble in dichloromethane (up to 300 mg in 0.5 mL) and could be characterized by ^{119}Sn NMR. Crystallizations were performed in dioxane containing 0.5% of water.[27] A 2 mL portion of dioxane was used for each 1 g of crude product. The dioxane solutions were cleared by heating at 85 °C and then returned slowly to room temperature and left still for a few days. A clean crystallization was not obtained for all experiments (i.e., the crystals were mixed with a fine powder). Crystals were isolated by filtration (fritted glass No. 2) and washed with about 50 mL of dioxane. Finally, crystals were dried overnight at 80 °C to yield compound **1**. Yields for various conditions are reported in Table 4.

1·diox. Anal. Found: Sn, 49.4; C, 27.3; H, 4.6; S, 2.2. Calcd for $Sn_{12}C_{62}H_{128}O_{26}S_2$·$C_4H_8O_2$: Sn, 49.69; C, 27.65; H, 4.79; S, 2.24. See Table 3 for ^{119}Sn, ^{1}H, and ^{13}C NMR data.

1. Anal. Found: Sn, 51.0; C, 26.8; H, 4.7; S, 2.4. Calcd for $Sn_{12}C_{62}H_{128}O_{26}S_2$: Sn, 51.27; C, 26.80; H, 4.65; S, 2.30. See Table 3 for ^{119}Sn NMR data.

Crystallography. Samples suitable for single-crystal X-ray diffraction were obtained by recrystallizing compound **1** in dioxane with less than 0.1% of water. Intensity data for the colorless crystal of **1**·diox were collected at room temperature on a Enraf-Nonius CAD4 diffractometer fitted with a graphite monochromator (Mo Kα radiation; $\lambda = 0.71069$ Å). The crystal was sealed in a Lindemann glass capillary tube. Details concerning the crystallographic data collection and structure determination are given in Table 5. Cell dimensions were determined from 25 reflections ($13.9 < \theta < 14.3°$) dispersed in reciprocal space. Two standard reflections were monitored every 2 h during data collection and showed less than 10% decay, which was nevertheless corrected, assuming a linear variation. Intensities were corrected for Lorentz and polarization effects, and an empirical absorption correction was applied.[28] The structure was solved using direct methods with the SHELXS program.[29] Successive Fourier maps were used to locate all non-H atoms and some H atoms (those of the PTS^-, those on the carbon atoms of butyl chains with small displacement parameters, mainly C_α and C_β, and two of the three bridging hydroxy groups (O45 and O56)). The other H atom positions were computed from the expected geometry of sp^3 CH_2 and CH_3. Full-matrix least-squares refinement, based on *F*, of atomic parameters and anisotropic thermal parameters for non-H atoms and of isotropic thermal parameters only for H atoms were carried out with CRYSTALS programs.[30] For H atoms, only two isotropic thermal parameters were considered: one for H atoms of μ_2-OH groups and one for all other H atoms. The atomic scattering factors were provided by CRYSTALS.[30] Final refinement details are given in Table 5. The numbering scheme employed is shown in Figure 1. The oxygen atoms inside the clusters are numbered with respect to the tin atoms they are bound with: e.g., O126 is bound to Sn1, Sn2, and Sn6 (or their symmetric counterparts) and O46 is bound to Sn4 and Sn6. The oxygen atoms of the sulfonate are numbered with respect to the μ_2-OH they are hydrogen-bound to: e.g., O45X is hydrogen-bound to O45.

Table 5. Crystallographic Data and Refinement Details for 1·diox

formula	$Sn_{12}C_{66}H_{136}O_{28}S_2$
M_r	2866.7
cryst color, habit	colorless, ∼parallelepiped
cryst size	$0.5 \times 0.3 \times 0.3$ mm^3
cryst syst	triclinic
space group	$P\bar{1}$ (No. 2)
unit cell dimensions	
a	12.722(3) Å
b	14.070(2) Å
c	16.014(3) Å
α	114.00(1)°
β	96.62(2)°
γ	104.24(1)°
V	2462(24) Å^3
Z	1
D_c	1.93 g cm^{-3}
F(000)	1388
diffractometer	Enraf-Nonius CAD-4
radiation (*λ*)	Mo Kα (0.71069 Å); graphite monochromator
μ	31.0 cm^{-1}
T	room temp
scan type	$\omega-2\theta$
scan width	$(0.8 + 0.345 \tan \theta)°$
θ range for data collecn	1−25°
hkl ranges	−15 to +15; −16 to +15; 0−19
no. of rflns collected	8984
no. of unique rflns	8645 ($R_{int} = 0.0192$)
abs correction	DIFABS (min: 0.89; max: 1.15)
no. of data/restraints/params	5927 [$I > 3.00\sigma(I)$]/0/490
refinement method	full-matrix least squares on *F*
secondary extinctn param $\times 10^6$	34.0
final indices:[a] *R*; R_w ($w = 1$)	0.0326; 0.0340
goodness of fit on *F*	2.16
residual electron density, min/max	−0.56/+0.70 e Å^{-3}

[a] $R = \Sigma||F_o| - |F_c||/\Sigma|F_o|$; $R_w = [\Sigma(w|F_o - F_c|^2)/\Sigma(wF_o^2)]^{1/2}$.

Thermal Analysis. Thermogravimetric and differential thermal analyses were carried out simultaneously, on a Netzsch STA 409 apparatus, using 50−100 mg of product in an alumina crucible, a pure oxygen atmosphere, and a 10 °C/min heating ramp from 20 to 1100 °C.

Conductivity Experiments. Measurements were performed in a thermostated (25 ± 0.05 °C) vessel with a Tacusel CD 810 conductimeter equipped with a Philips cell. The cell constant was determined prior to each series of measurements with a potassium chloride solution (10^{-2} mol/L) of known ionic conductivity. The measurements were performed for concentrations from 5×10^{-3} to 5×10^{-2} mol/L in CD_2Cl_2 or DMSO.

Solid-State ^{119}Sn MAS NMR Experiments. The ^{119}Sn MAS (magic angle spinning) NMR experiments have been

(27) The use of anhydrous dioxane (less 0.1% of water) resulted in an incomplete crystallization, as evidenced by lower yields. The use of dioxane with 1% of water resulted in a faster, but unclean, crystallization. Therefore, dioxane with 0.5% of water was preferred for crystallizing **1**·diox**.**

(28) Walker, N.; Stuart, D. *Acta Crystallogr., Sect. A* **1983**, *39*, 158.

(29) Sheldrick, G. M. SHELXS-86, Program for Automatic Solution of Crystal Structure; University of Göttingen, Göttingen, Germany, 1986.

(30) Watkin, D. J.; Prout, C. K.; Carruthers, J. R.; Betteridge, P. W. CRYSTALS issue 10; Chemical Crystallography Laboratory, University of Oxford, Oxford, U.K., 1996.

performed on a Bruker MSL300 spectrometer (111.92 MHz for ^{119}Sn) equipped with a 4 mm high-speed locked Bruker probe. The spectral width was 200 000 Hz (~1800 ppm); pulse angles and recycling delays were about 30° (1.5 μs) and 10 s, respectively. Longer recycling delays (up to 30 s) gave identical quantification within experimental error. Moreover, for compound **1** the longitudinal relaxation time (T_1) was measured by saturation recovery around 10 and 17 s for five- and six-coordinate tin atoms, respectively. Typically 1000−5000 transients were necessary to achieve reasonable signal-to-noise ratios. ^{119}Sn chemical shifts are quoted relative to Me_4Sn, using solid tetracyclohexyltin (δ_{iso} −97.35 ppm) as a secondary external reference.[32] At least two experiments, with sufficiently different spinning rates, were run in order to identify the isotropic chemical shifts. The spinning frequencies were stabilized to ±5 Hz.

The solid-state NMR experiments with a Hahn echo have been carried out using a Bruker DSX 300 spectrometer operating at 7.04 T with a Larmor frequency of 111.92 MHz for ^{119}Sn. The MAS spectra were acquired using a rotor-synchronized Hahn echo sequence ($\theta-\tau-2\theta-\tau-$acq; with $\theta \approx 30°$ and $\tau = 1/\nu_{MAS}$, ca. 74 μs for 13 500 Hz). The pulse durations were limited to 2 μs in order to ensure complete excitation of the spectra. The recycling delay was set to 70 s for compound **1** and to 60 s for the crude product. The spinning frequency was stabilized to ±10 Hz. Chemical shifts were referenced to tetramethyltin, using a solution of **1** in CH_2Cl_2 as a secondary external reference.

The principal components of the ^{119}Sn shielding tensors were analyzed with WINFIT software[33] using the Herzfeld and Berger approach.[34] They are reported, following Haeberlen's notation,[35] as the isotropic chemical shift ($\delta_{iso} = -\sigma_{iso}$), the anisotropy ($\zeta = \sigma_{33} - \sigma_{iso}$), and the asymmetry ($\eta = |\sigma_{22} - \sigma_{11}|/|\sigma_{33} - \sigma_{iso}|$), σ_{11}, σ_{22}, and σ_{33} being the three components of the shielding tensor expressed in its principal axis system with the following convention: $|\sigma_{33} - \sigma_{iso}| \geq |\sigma_{11} - \sigma_{iso}| \geq |\sigma_{22} - \sigma_{iso}|$.[15] With this convention, ζ is a signed value expressed in ppm and η is a dimensionless parameter, the value of which is between 0 and 1. The accuracy on δ_{iso}, ζ, and η corresponds to the digital resolution (±0.5 ppm), ±10 and ±0.05 ppm, respectively.

Solution NMR Experiments. Routine ^{119}Sn, ^{1}H, and ^{13}C NMR experiments were performed on a Bruker AC300 spectrometer (300.13, 111.92, and 75.47 MHz for ^{1}H, ^{119}Sn, and ^{13}C, respectively). Proton-decoupled ^{119}Sn NMR spectra were obtained with a composite pulse decoupling sequence (WALTZ), and ^{119}Sn chemical shifts are relative to external tetramethyltin. ^{1}H and ^{13}C chemical shifts were referenced to the residual solvent peak (CD_2Cl_2) and converted to the standard $SiMe_4$ scale by adding 5.32 and 53.3 ppm for ^{1}H and ^{13}C nuclei, respectively.

Quantitative ^{119}Sn NMR experiments were performed as follows. The ^{119}Sn NMR spectra of samples made of a precisely weighed amount of crude product (ca. 100 mg) in 0.5 mL of CD_2Cl_2 were recorded (1500 transients) without proton decoupling to avoid NOE effects. The recycling delay was 3 s, far above the longitudinal relaxation time (T_1) of both ^{119}Sn environments, which were measured around 0.15 and 0.20 s for five- and six-coordinate tin nuclei, respectively. Their integrations, in absolute mode, were compared to a reference obtained the same day, under the very same experimental conditions, from a tube containing 100 mg of compound **1** and 0.5 mL of CD_2Cl_2. The linearity of the measurement was assessed with sample tubes containing various known amounts of compound **1**. The integral of each resonance (−283 and −462 ppm) gives the same results within 5%, which can be considered as the accuracy of the method.

The proton-detected 2D ^{1}H−^{119}Sn HMQC experiment was recorded at 303 K on a Bruker AMX500 spectrometer, interfaced with a Silicon Graphics O2 computer, operating at 500.13 and 186.50 MHz for ^{1}H and ^{119}Sn, respectively, without ^{119}Sn decoupling, using the pulse sequences of the Bruker library[36] adapted to include gradient pulses,[37] as proposed and illustrated recently.[19,38]

The phase-sensitive ROESY and NOESY spectra[18,19] were recorded from pulse sequences of the standard Bruker library, at variable mixing times with 4K × 512 data matrices (F1 zero-filled to 1K). Distances separating protons were calculated from the intensity of the corresponding cross-peaks, using the distance between two protons in mutually ortho positions as an internal reference (2.48 Å)[22] and the equation $r_i = r_{ref}(k_{ref}/k_i)^{1/6}$.[17,20,21] In this equation r_i represents the interatomic distance of interest and r_{ref} the reference distance, while k_{ref} and k_i are the slopes of the respective build-up straight lines in the ROESY spectra,[17,20,21] in the initial rate approximation, associated with the cross-peaks mutually correlating the pairs of nuclei under consideration. The above formula only holds if the reference pair and the pair of protons of interest are subject to comparable rotational tumbling regimes.[20,21] The 2D ROESY experiments were performed with mixing times of 400, 600, and 800 ms in CD_2Cl_2 and with mixing times of 300, 600, and 900 ms in DMSO-d_6 (both at 303 K). The 2D NOESY experiments in DMSO-d_6 were performed with mixing times of 400, 600, and 800 ms at 303 K. The volumes of the cross-peaks were used in the calculation instead of the slopes of the build-up straight lines to which they are in principle proportional, to avoid time-consuming build-up experiments.

The ^{1}H−^{119}Sn *J*-HMQC spectra were recorded with the pulse sequence of Willker and Leibfritz,[24] adapted with the gradient pulse schemes previously proposed for ^{1}H−^{119}Sn HMQC spectroscopy.[19,38b] The ^{119}Sn frequency carrier was set on resonance at the frequency of the six-coordinate tin atom. A total of 32 delays were used for total preparation periods of 620 ms in CD_2Cl_2 and of 310 ms in DMSO-d_6. The *J*-HMQC technique is essentially an HMQC experiment in which a 180° pulse is applied between two identical but increasingly incremented time delays, embedded in a preparation period which is kept constant.[24] This introduces a sine modulation in the amplitude of the finally detected ^{1}H−^{119}Sn HMQC correlation, which is determined by the incremented delay and the coupling constant to be measured. This sine-modulated signal amplitude is not affected by relaxation damping. The desired coupling constant is then simply extracted from curve fitting of the experimentally generated sine function. Methodological and theoretical details as to the implementation of this technique to the ^{119}Sn nucleus, with gradient pulses, will be published elsewhere.[25] The confidence intervals given with the $^2J(^1H-O-^{119}Sn_h)$ coupling constant values represent the standard deviation on the mean values found from two independent experiments for each solvent (CD_2Cl_2 and DMSO-d_6).

(31) Watkin, D. J.; Prout, C. K.; Pearce, L. J.; CAMERON; Chemical Crystallography Laboratory, University of Oxford, Oxford, U.K., 1996.
(32) Reuter, H.; Sebald, A. *Z. Naturforsch.* **1992**, *48B*, 195.
(33) Massiot, D.; Thiele, H.; Germanus, A. *Bruker Rep.* **1994**, *140*, 43.
(34) Herzfeld, J.; Berger, A. E. *J. Chem. Phys.* **1980**, *73*, 6021.
(35) Haeberlen, U. *Adv. Magn. Reson.* **1976**, Suppl. 1.
(36) Bax, A.; Griffey, R. H.; Hawkins, B. L. *J. Magn. Reson.* **1983**, *55*, 301.
(37) (a) Keeler, J.; Clowes, R. T.; Davis, A. L.; Laue, E. D. *Methods Enzymol.* **1994,** *239*, 145. (b) Tyburn, J.-M.; Bereton, I. M.; Doddrell, D. M. *J. Magn. Reson.* **1992**, *97*, 305. (c) Ruiz-Cabello, J.; Vuister, G. W.; Moonen, C. T. W.; Van Gelderen, P.; Cohen, J. S.; Van Zijl, P. C. M. *J. Magn. Reson.* **1992**, *100*, 282. (d) Vuister, G. W.; Boelens, R.; Kaptein, R.; Hurd, R. E.; John, B. K.; Van Zijl, P. C. M. *J. Am. Chem. Soc.* **1991**, *113*, 9688.
(38) (a) Kayser, F.; Biesemans, M.; Gielen, M.; Willem, R. *J. Magn. Reson.* **1993**, *A102*, 249. (b) Martins, J. C.; Kayser, F.; Verheyden, P.; Gielen, M.; Willem, R.; Biesemans, M. *J. Magn. Reson.* **1997**, *124*, 128. (c) Kayser, F.; Biesemans, M.; Gielen, M.; Willem, R. In *Advanced Applications of NMR to Organometallic Chemistry*; Gielen, M., Willem, R., Wrackmeyer, B., Eds.; Wiley: Chichester, U.K., 1996; Chapter 3, pp 45−86.

Acknowledgment. We acknowledge Drs. J. Vaissermann and F. Robert for their help with the X-ray structure, J. Maquet for her precious assistance in solid-state ^{119}Sn MAS NMR, G. Dureau and C. Parussolo for their experimental work, and Eng. I. Verbruggen for technical assistance in NMR acquisitions. F.R., C.S., M.B., and R.W. are indebted to the European Union Program "Human Capital and Mobility" for financial support (Contract No. ERBCHRX-CT-94-0610). M.B. and R.W. are indebted to the Fund for Scientific Research Flanders (Belgium, Grant No. G0192.98) for financial support. F.R., C.S., M.B., and R.W. are indebted to the Flemish Ministry of Education and the French Ministries of Foreign Affairs and Education, Research and Technology for the allocation of a Tournesol Grant (No. 99 091). J.C.M. is a postdoctoral fellow of the fund for Scientific Research Flanders (Belgium, FWO).

Supporting Information Available: Further details of the structure determination, including bond distances and angles and thermal parameters for $\{(BuSn)_{12}O_{14}(OH)_6\}(4\text{-}CH_3C_6H_4SO_3)_2 \cdot C_4H_8O_2$ (**1**·diox). This material is available free of charge via the Internet at http://pubs.acs.org.

OM990877A